

# Remote Sensing Techniques in Disaster Management: Amynteon Mine Landslides, Greece



Aikaterini Karagianni, Ilias Lazos and Alexandros Chatzipetros

**Abstract** Natural or man-made disasters are phenomena that can affect large areas and have many environmental, societal and economic impacts. Landslides are among the major disasters of large scale that may affect the natural environment as well as urban areas, often causing massive destruction, loss of property, or even fatalities worldwide. Developing tools that are effective for disaster management is imperative to monitor and mitigate their effect. Satellite data and remote sensing techniques, combined with geological data and studies can provide valuable information regarding monitoring of natural hazards in general and especially of landslides. This chapter concerns the ex ante and ex post study of a complex set of landslides that occurred in the lignite mine of Amynteon in north-western Greece (June 2017). Weakened material cohesion due to fragmentation, further degraded by mining activities and hydrogeological factors led to the catastrophic event. The landslide occurred in along the south faces of the mine, resulting to extended collapses, destruction of mining machinery, evacuation of the adjacent Anargyri village and a big financial impact. Landsat 8 and Sentinel-2 satellite data acquired before and after the event are being used. Digital image processing techniques are applied for change detection. In addition, geological data are being used to provide information about the geological background of the area and landslides vulnerability. Visual interpretation of the area affected by the landslides is also being done, contributing to the overall study.

---

A. Karagianni (✉)

Laboratory of Photogrammetry – Remote Sensing, School of Civil Engineering,  
Faculty of Engineering, Aristotle University of Thessaloniki, Thessaloniki, Greece  
e-mail: [aikateck@civil.auth.gr](mailto:aikateck@civil.auth.gr)

I. Lazos · A. Chatzipetros

Laboratory of Geology and Palaeontology, School of Geology,  
Aristotle University of Thessaloniki, Thessaloniki, Greece  
e-mail: [ilialazo@geo.auth.gr](mailto:ilialazo@geo.auth.gr)

A. Chatzipetros

e-mail: [ac@geo.auth.gr](mailto:ac@geo.auth.gr)

© Springer Nature Switzerland AG 2019

O. Altan et al. (eds.), *Intelligent Systems for Crisis Management*,  
Lecture Notes in Geoinformation and Cartography,  
[https://doi.org/10.1007/978-3-030-05330-7\\_9](https://doi.org/10.1007/978-3-030-05330-7_9)

## 1 Introduction

Natural or man-made disasters are phenomena that can affect large areas and have many environmental, societal and economic impacts (van Westen 2000). Landslides are among the major disasters of large scale that may affect the natural environment as well as urban areas. The occurrence of destructive landslide phenomena is frequent worldwide, causing radical changes in the wider area, related to geomorphological, environmental, societal and economic factors (Metternicht et al. 2005).

Landslide hazard of an area is an essential parameter in the overall assessment of the geological-geotechnical suitability of this area. Activation of landslide phenomena is connected to a variety of endogenous and exogenous factors. Most land slopes have reached a state of equilibrium as it has been formed during the geological evolution of the slopes (discharges due to erosion, change in material properties, old movements, etc.).

Mass movements are the result of many and complex processes that present a dynamic development and cause significant environmental degradation. The extent and rate of environmental impacts range from the morphological evolution of the surface due to geodynamic erosion processes to the local and rapid change of topographic data of an area, caused by a landslide. According to their characteristics (materials involved and mode of movement), landslides can be classified in various types that often determine the study approach.

Landslides are primarily associated with mountainous regions. However, they can also occur in areas of generally low relief as cut-and-fill failures (roadway and building excavations), collapse of mine-waste piles (especially coal), river bluff failures, lateral spreading landslides and a wide variety of slope failures associated with quarries and open-pit mines (USGS 2018).

Monitoring landslide activity over extensive areas occurs as an important aspect at the management of natural hazards and risk. Detection and monitoring of landslide areas, in order to understand their dynamics, could provide useful information regarding negative effects reduction (Gili et al. 2000). Especially in areas of natural resources extraction, studying of these phenomena is quite important and necessary as it is connected to a combination of factors and impacts (Paull et al. 2006).

Landslide monitoring could be accomplished by several methods (Hervás et al. 2003). Among the used methods, satellite data and remote sensing techniques can be proven of particular importance as they provide wide coverage of the affected areas, high frequency data and information about non-visible spectral regions (Mantovani et al. 1996; Scaioni et al. 2014; Joyce et al. 2009). Additional geological data can provide information about the geological background of the area contributing in landslide disaster management studies (Scaioni et al. 2014).

In general, remote sensing data offer valuable information during various phases of a landslide study as: detection and classification of landslides, monitoring the activity of existing landslides, analysis and prediction in space and time of slope

failures (Mantovani et al. 1996). Particularly in landslide monitoring, a wide range of satellite remote sensing techniques in combination with more traditional or recently developed methods can be applied to obtain useful data (aerial or terrestrial photogrammetry, Global Position System for location determination, thermal infrared data for soil moisture conditions monitoring in relation to landslide movements, etc.).

Regarding monitoring of landslides in mine areas, remote sensing data are able to provide information on changes in local environments in a cost effective way. Furthermore, this type of data has been successfully used in several cases of mining sector studies as investigating geological hazards or monitoring the environmental impact of mining (Wang et al. 2013; Paull et al. 2006; Li et al. 2015; Dong et al. 2009). In combination with other forms or sources of data (e.g. geological data, terrestrial imagery, precipitation data sets, surface displacement measurements), remote sensing data may contribute to the assessment of changes in land cover, the extent of the physical impact of mining operations (e.g. infrastructure, mining pits, sedimentation), the effects of migration and settlement dynamics, etc. (Paull et al. 2006). Satellite images offer quick and concise views of a potential geological hazard area, composing a large database that presents the dynamic changes caused by landslide phenomena and thus can be a valuable and efficient tool in mine monitoring (Wang et al. 2013).

The case study presented in this chapter concerns a large scale landslide phenomenon that took place in June 10, 2017 in the lignite mine of Amynteon, region of Western Macedonia in Greece, leading to the destruction of a large part of the mine, cancelation of mining activities, partial destruction and evacuation of the adjacent Anargyri village and multiple socio-economic impacts. Landsat 8 and Sentinel-2 satellite data acquired before and after the event are being used. Digital image processing techniques are applied for change detection and visual interpretation of the area affected by the landslides is also being done. In addition, an overview of the geological structure and the tectonic setting of the active faults of the area, as well as the landslide type and its triggering factors are presented.

## 2 Study Area

Study area is located in the north-western part Greece, region of Western Macedonia, in medium-high altitude (600 m) and concerns the lignite mine of Amynteon. The mine is located between lakes Vegoritis and Chimaditis, close to the town of Amynteon. The smaller village of Anargyri is located on the southwest side of the mine. Figure 1 presents the location of the study area in Greece (red dot), as well as a satellite image of the mine from Google Earth (2018).

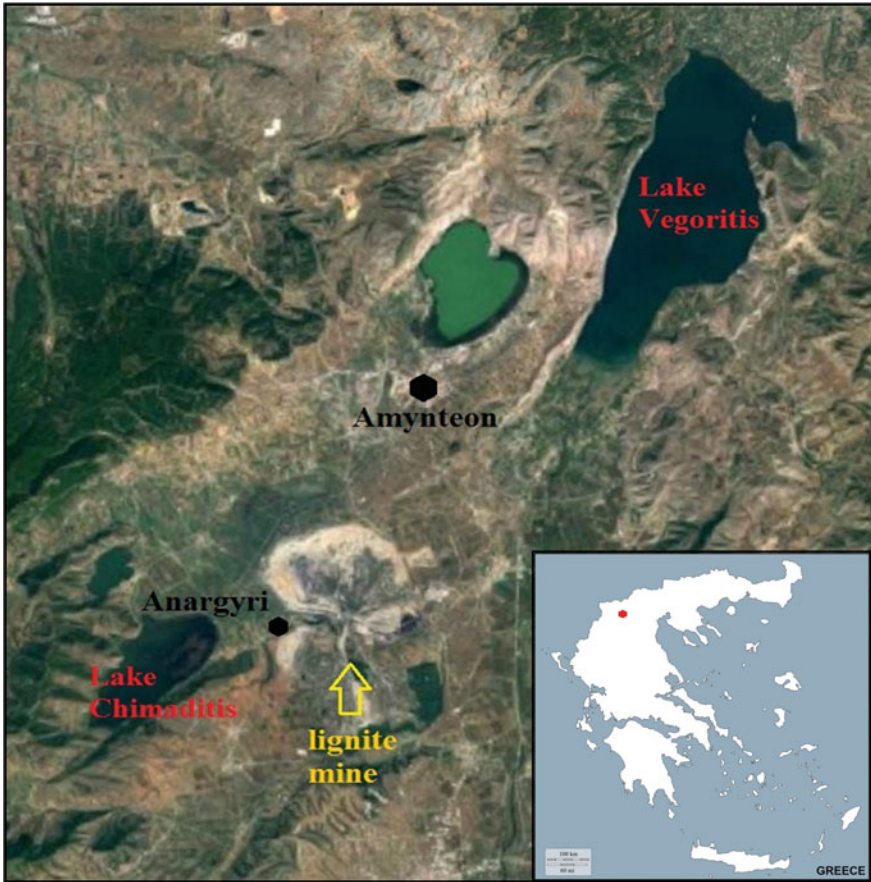


**Fig. 1** Location of the study area in Greece (red dot) and satellite image of the mine from Google Earth

### 3 Geological and Structural Setting

#### 3.1 Geological Setting

The bedrock of the broader area is comprised mainly of Pelagonian geological zone and, covering a much smaller area, Subpelagonian rocks. In general terms, Palaeozoic metamorphic rocks are overlain either stratigraphically or tectonically by younger Mesozoic and Tertiary rocks (Mountrakis 1986). The bedrock is unconformably covered in places by post-alpine sedimentary formations, while Upper Quaternary deposits (mainly alluvium and scree) cover locally both of them. The Pelagonian bedrock is mainly structured in four distinct units (Mountrakis 1986; Pavlides and Mountrakis 1987): (a) Palaeozoic crystalline rocks, including

granite intrusions and Permian-Triassic metaclastic sequences, (b) Triassic-Jurassic carbonates, which constitute the main part of the bedrock in the study area, (c) ophiolites and associated sediments, overthrusting Pelagonian zone and (d) Middle-Late Cretaceous transgressive sediments. Most of the study area is covered by mainly lacustrine Middle Pliocene–Lower Pleistocene sediments. The Pliocene formation comprises of three main horizons: the lower one is dominated by conglomerate, containing ophiolitic clasts, red clay and marls. A middle horizon comprises of fine-grained sediments, mainly white marl, with thin lignite-bearing layers. The uppermost horizon contains alternations of white marl and marly limestone with occasional sandy layers. The total thickness of the Pliocene deposits is more than 700 m at the central part of the basin. The Lower Pleistocene sequence is rather cohesive and consists of red clays with gravel parts at its lower part and red clay and breccia at its upper one (Pavlidis and Mountrakis 1987).

### 3.2 *Structural Setting*

The area of NW Greece has been subjected to several deformations, which caused continuous geomorphological changes and a variety of tectonic structures (active or not). Successive deformation phases affected in various ways the geotectonic evolution of the area, forming its current structure (Kilias and Mountrakis 1989). The first major deformation phase is associated with the thrusting of Axios (Vardar) and Subpelagonian ophiolites. They overthrust the Pelagonian carbonates and are associated with the destruction of the Axios and Subpelagonian-Pindos oceans. This phase is imprinted on the schistosity and folding and is characterized by abundant ophiolitic mélangé (Figs. 2 and 3). The Upper Cretaceous–Upper Eocene compressional phase formed NW-SE trending folds and thrusts. This imbrication caused widespread inversions, especially along the western Pelagonian margin. The major folding resulted in the formation of NW–SE trending anticline and syncline structures.

An ENE-WSW trending extensional event during the Lower Oligocene formed the molassic Mesohellenic Trench (Figs. 4 and 5). The detachment faults of this phase affected the ophiolite masses under semi-ductile conditions, causing their displacement to approximately their current location. The 40-km-wide Mesohellenic Trench is developed in a NNW-SSE direction, transversely to the direction of Lower Oligocene extension, constituting the most recent and extensive molassic trench of Greece, while the sedimentation went on from Oligocene to Upper Miocene. During the Middle–Upper Miocene, an E-W compressional phase caused the formation of N-S trending ophiolite imbrications, as well as strike-slip faults of WNW–ESE strike. A significant number of them were reactivated as normal faults during the subsequent extensional neotectonic phases. The compressional deformation was completed during the Upper Miocene by the last NNE-SSW trending phase. This phase formed E-W reverse faults in the ophiolitic masses and reactivated of the inherited strike-slip faults.



**Fig. 2** Ophiolitic mélangé of the broader area, derived from the Axios and Subpelagonian-Pindos oceans destruction (later generation quartz veins crisscross the rock mass)



**Fig. 3** Characteristic example of a slickenside in the broader area (successive stages of brittle, semi-brittle & ductile deformation are evident throughout the ophiolitic mass)



**Fig. 4** Molassic formations (alternations of sandstones and marls) of the Mesohellenic Trench of the broader area



**Fig. 5** Reverse fault in the molassic formations of the Mesohellenic Trench

### ***3.3 Neotectonic Setting***

Two main neotectonic extensional phases affected the broader NW Greece area (Pavlidis 1985; Pavlidis and Mountrakis 1987). The first one, during Upper

Miocene–Pliocene, created or reactivated NW-SE trending normal faults, which formed large grabens of the same direction. A constant NE-SW directed extensional stress field affected the entire interior Aegean region. The last deformation phase during the Quaternary is still active. This NNW-SSE trending extension caused the formation or reactivation of significant NE-SW to E-W striking normal faults. They caused the fragmentation of the large grabens into smaller transverse sub-basins. This extensional phase is currently active and its faults played the most important role in the neotectonic evolution of the area. Several of these NE-SW to ESE-WNW striking faults have been active during the Neogene-Quaternary and are located within the large basins of the area (Florina, Amynteon–Ptolemais and Kozani ones). One of the most important faults in the area is the Aliakmon one, a segment of which was activated during the May 13th, 1995 Kozani-Grevena Mw 6.6 earthquake (Pavlidis et al. 1995; Chatzipetros 1998). Nevertheless, several earthquakes of smaller magnitude have been recorded in the broader area (Tsapanos 2005). Figure 6 presents the Neotectonic faults and epicenter locations of earthquake events within the time period 1800–2007 into the broader area (modified from Tsapanos 2005). Several microseismic events are recorded in the close area of the main active tectonic structures.

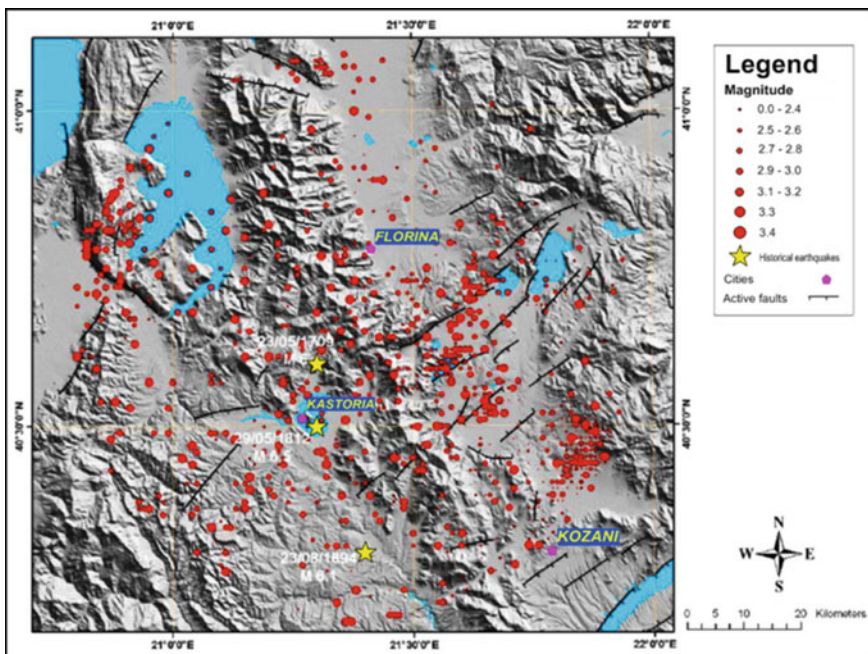


**Fig. 6** Neotectonic faults and epicenter locations of earthquake events within the time period 1800–2007 into the broader area (modified from Tsapanos 2005)



### 3.4 Active Faults of the Study Area

The broader Ptolemais basin, where the lignite mine of Amynteon is located, is characterized by six major active fault zones (Fig. 7). They are Komnini-Asvestopetra (possibly extended to Pyrgi village), Emporion-Perdika, Anargyri (or Chimaditida-Anargyri), Perea-Maniaki, Vegora (or Vegoritida-AgiosPanteleimon) and Nymfeon-Xino Nero-Petres Lake (Pavlidis 1985). The Amynteon mine landslide is associated to Anargyri and Vegora active faults. Nevertheless, a multitude of secondary faults also affect the area of the mine and might have contributed to the weakening of the rock/soil mass (see Tzampoglou and Loupasakis 2018 and references therein).

#### 3.4.1 Anargyri Fault

Anargyri fault is one of the major faults of Amynteon-Ptolemais basin and defines the southern shore of Chimaditida Lake (Pavlidis 1985). It is of N60E strike and dips to the NW. It forms the Chimaditida Lake graben, which is the most recent (Quaternary) graben of the basin. Based on drilling data from the lignite-bearing sediments, the estimated fault throw is 130 m. The Anargyri fault affects the entire Pliocene-Quaternary sequence.

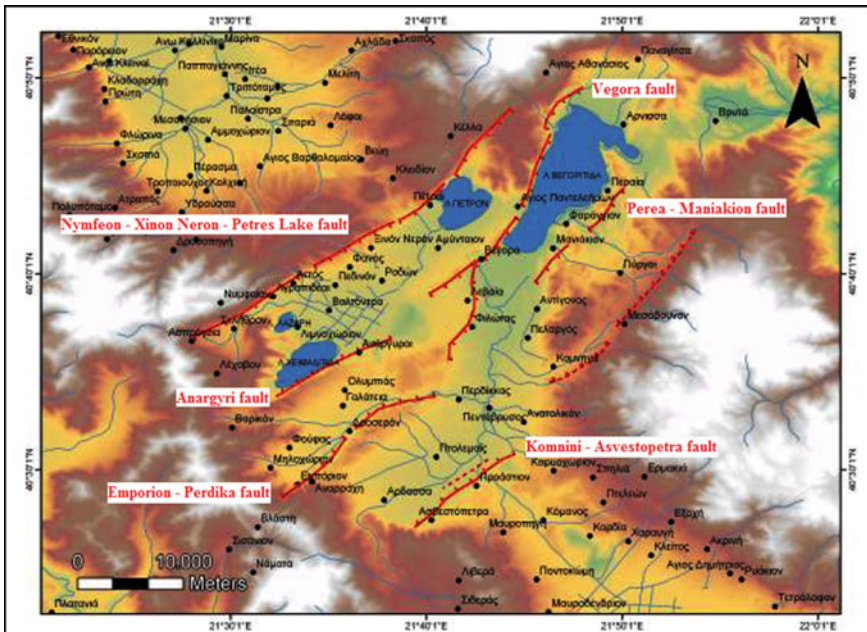


Fig. 7 Simplified structural map of the study area (modified from Pavlidis, 1985)

### 3.4.2 Vegora Fault

Vegora fault is a major normal fault along the western shore of Vegoritida Lake, with a NE-SW strike (between  $30^\circ$  and  $40^\circ$ ), while the estimated dip angle is  $60^\circ$  SE (Pavlidis 1985). The total length of Vegora fault is 20 km, and it deforms the Mesozoic Pelagonian carbonates, forming the Vegoritida Lake graben. A SW extension of this fault zone extends into the Pliocene and Quaternary sediments of Ptolemais basin, while the fault throw is estimated between 200 and 500 m. It is also considered an active fault, as it deforms very recent scree that overlies the fault slickenside.

### 3.5 Interpretation of the Tectonic Setting of the Amynteon Lignite Mine Area

The interaction of both the Anargyri and Vegora faults affects the Amynteon lignite mine area, leading to complicated deformation of the lignite-bearing formations, forming a transitional transfer zone.

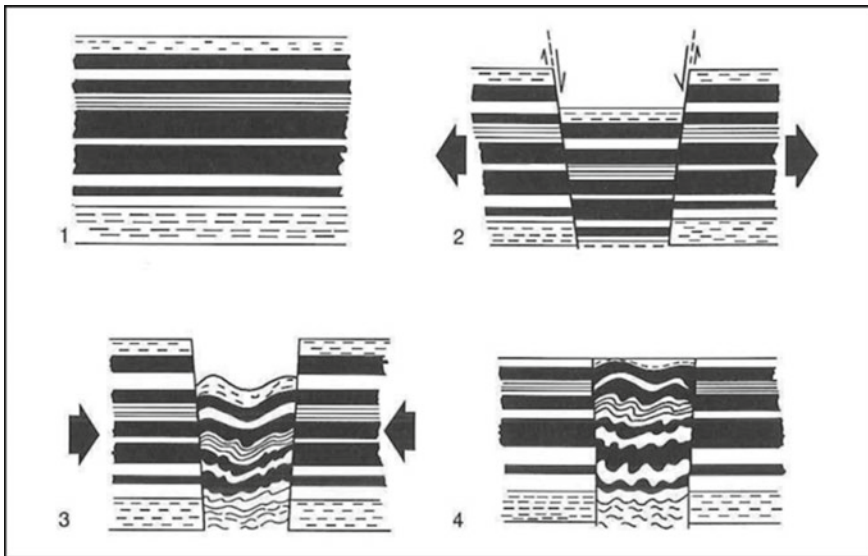


**Fig. 8** Schematic representation of the subsequent stages of a pincée structure: (1) Deposition of horizontal beds, (2) Graben formation (extensional stage), (3) Folding of the graben formations (compressional stage), (4) Final form due to erosion (modified from Pavlidis 1985)

Furthermore, various tectonic structures are observed within the mine. The most important of them are normal faults, which are dominant, but also bed-parallel slip, anticlines, reverse faults, folds and grabens. All these structures can be produced by the interplay of localized extensional and compressional tectonic processes, often forming what is known as pincée structures. A pincée structure is characterized by the formation of a graben in an initial stage (extensional stage), while a subsequent compressional one, which can be very weak, folds the formations within the graben (Fig. 8).

## 4 The Amynteon Mine

Amynteon mine is one of the main lignite mining areas in the broader Ptolemais basin coal field. Mining produces lignite which is used for power production in the adjacent Amynteon coal power plant. Throughout the years, the mine has experienced successive expansions both horizontally, as well as vertically. This was necessary in order to respond to increased demand, as well as to follow the coal seams that are being displaced by numerous faults.

Figure 9 presents a typical excavation front, exhibiting a very complex faulting pattern, causing the lignite seams and the intercalated marl to fracture and be deformed by occasionally large displacements. This multifractured nature of the sequence might have played a role in reducing the cohesiveness of the material and hence facilitated the landslide.



**Fig. 9** Typical excavation front of the Amynteon lignite mining area

### 5 The Amynteon Mine Landslides

Landslides are some of the most important destructive phenomena and are caused by both natural and man-made factors. Landslides are classified into several types, the main ones being (a) rotational, (b) translational, (c) block slide, (d) rockfall, (e) toppling and (f) creep. The Amynteon lignite mine landslide shows characteristics of a rotational landslide. According to U.S. Geological Survey (USGS 2018),

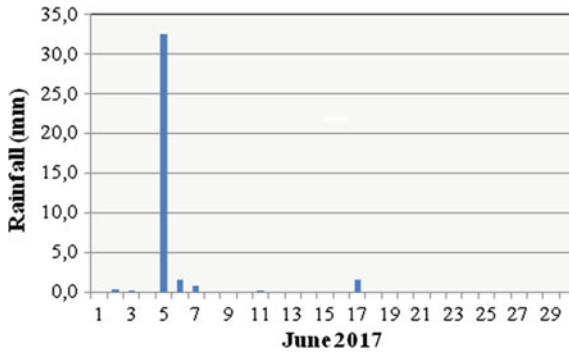


Fig. 10 Rainfall during June 2017



Fig. 11 General view of the June 10, 2017 Amynteon mine landslide

rotational landslide is a slide in which the surface of rupture is curved concavely upward and the slide movement is roughly rotational about an axis that is parallel to the ground surface and transverse across the slide. Furthermore, this type of landslide is observed mainly into soil masses, while other landslide types (block slide, rockfall and topple) are common in cohesive rock formations.

The exact failure factors have not been determined yet and are subject to ongoing modelling (e.g. Tzampoglou and Loupasakis 2017a, b; 2018; Dimitrakopoulos and Koumantakis 2017), as well as investigation by expert panels appointed by the Ministry of Infrastructure, Transport and Networks and the owner of the mine (Public Power Company S.A.). It is possible that the Plio-Pleistocene sedimentary sequence in Amynteon mine acted as a soil mass, due to the intense fragmentation caused by extensive faulting and jointing associated to the transfer zone between Anargyri and Vegora faultzones. These faults affected the lignite bearing formations, causing poor cohesion and leading to the formation of a multifragmented mass. Furthermore, it is



**Fig. 12** Ground rupture at Anargyri village due to the landslide

possible that human factors affected the initiation of the landslide. The deep excavation at the foot of the mining fronts and the simultaneous deposition of material at the mine's upper part may have charged the upper excavation area, while the stability at the lower part was reduced. Initial signs of failure (e.g. creep, surface ruptures, etc.) caused halting of mining activity at this sector and removal of machinery. Finally, a few days before the main landslide a rather extreme rain event was recorded (36.2 mm of precipitation) during a normally dry period. Figure 10 presents a diagram based on rainfall data of the area during June 2017 (Interactive database Meteosearch 2018).

The landslide effects covered a large area and caused damages in the order of several hundreds of millions of Euros, due to loss of exploitable lignite deposits, destruction of mining machinery and equipment, halting of works and significant damages to the nearby Anargyri village, a large part of which was preventively evacuated (Figs. 11 and 12). Compensation of properties and public infrastructure damaged during the landslide will also add further to the total cost.

## 6 Satellite Data

The constant evolution of technology in remote sensing and Earth observation provide continuous information, several times under the policy of free data. The available satellite data have significantly increased over the past years, offering various possibilities for a high number of applications.

The data employed for this case study concern Landsat 8 and Sentinel-2 satellite imagery acquired before and after the catastrophic event, providing the ability to detect the landslide and monitor the affected area, highlighting also the changes.

### 6.1 Landsat 8 Satellite Data

Landsat 8 was launched on February 11, 2013 and carries two instruments: The Operational Land Imager (OLI) sensor and the Thermal Infrared Sensor (TIRS). These sensors both provide improved signal-to-noise (SNR) radiometric performance, quantized over a 12-bit dynamic range (4096 potential grey levels in an image compared with only 256 grey levels in previous 8-bit instruments). Improved signal to noise performance enables better characterization of land cover state and condition (Landsat 8 Mission 2018).

Satellite data acquired from Landsat 8 consist of eleven spectral bands with a spatial resolution of 30 m for Bands 1–7 and 9. The resolution for Band 8 (panchromatic) is 15 m and for Bands 10, 11(thermal bands) is 100 m. Among the eleven spectral bands, Landsat 8 includes one band that measures the near infrared (Band 5-NIR) and two bands that cover different slices of the shortwave infrared (Bands 6 and 7-SWIR).

Landsat 8 satellite data could be a useful tool for monitoring and analysing the territory, as their spectral capabilities give the opportunity to identify the extent of the landslide and provide additional information about the landslide location and the affected area in general.

The image data that have been used in this study were downloaded free of charge from USGS EarthExplorer (2018). They were acquired at 2017-05-02 (path: 185, row: 32) and 2017-06-26 (path: 184, row: 32) before and after the landslide event respectively, with level processing 1T–Standard Terrain Correction (systematic radiometric and geometric accuracy) and projection information: UTM, zone 34, spheroid and datum WGS 84. The images have excellent quality (image quality: 9).

## 6.2 *Sentinel-2 Satellite Data*

Sentinel-2 mission consists of two polar-orbiting satellites (Sentinel-2A and Sentinel-2B) providing high-resolution optical imagery for land monitoring. The full mission specification of the twin satellites flying in the same orbit but phased at 180°, is designed to give a high revisit frequency of 5 days at the Equator. Among the mission objectives is the disaster relief support and change detection maps (Sentinel-2 Mission 2018).

Sentinel-2A was launched on June 23, 2015 while Sentinel-2B on March 07, 2017. Both satellites are equipped with the MSI (Multispectral Imager) instrument that offers high-resolution optical images. Sentinel-2 mission, as Landsat 8, is provided on board with an optical-multispectral high resolution sensor that operates on/covering 13 different bands: four visible and near-infrared bands with a spatial resolution of 10 m (bands 2, 3, 4, 8), six red edge and shortwave infrared bands with a spatial resolution of 20 m (bands 5, 6, 7, 8A, 11, 12) and three atmospheric correction bands with a spatial resolution of 60 m (bands 1, 9, 10). Sentinel data products are available to all users and can be accessed free of charge (free, full and open data policy adopted for the Copernicus programme) through the Copernicus Open Access Hub (2018).

The image data that have been used in this study derive from Sentinel-2A (S2A\_MSIL2A) and were acquired at 2017-06-01 and 2017-06-21 respectively with level processing 2A. The Level-2A products provide Bottom of Atmosphere (BOA) reflectance images derived from the associated Level-1C products. Each Level-2A product is composed of  $100 \times 100$  km<sup>2</sup> tiles in cartographic geometry (UTM/WGS84 projection).

## 7 Digital Image Processing

As a result of the several sensors that satellite platforms are equipped with, the obtained data are available in digital form. Digital images of spectral reflectance data give us the advantage to apply computer analysis techniques to extract information. Every discrete picture element (pixel) of a digital image is represented by a digital number (DN) which depicts the average radiance of relatively small area within a scene. Smaller numbers indicate low average radiance. Digital image processing is based on these numbers and includes computer based procedures that concern four basic operations: image rectification and restoration, image enhancement, image classification and data merging (Lillesand and Kiefer 1987).

Image rectification and restoration include operations dealing with correction and calibration of distorted images in order to achieve a more faithful representation of the original scene (e.g. radiometric and geometric corrections). This type of restoration preprocessing depends on the type of image format, the initial condition of the image and its level processing, as well as the information of interest and the composition of the image scene. These operations prepare data for subsequent analysis, although might not be necessarily applied in all case, as systematic errors can be removed before they reach the user (Navi 2017).

Image enhancement includes operations to improve the interpretability of an image for a particular application, by increasing the apparent contrast among various features in the scene. Accentuation of the contrast can increase the amount of information that can be visually interpreted (Lillesand and Kiefer 1987). Enhancement techniques are often used for feature extraction, making important features more interpretable to the human eye (ERDAS Field Guide 2013). Depending on the data, objectives, expectations and interpreter's background, several enhancement techniques can be applied to derive useful information from images by studying and locating areas or objects on the ground.

Image classification includes quantitative techniques that can be applied to automatically interpret digital image data. During this process, individual pixels are evaluated and assigned to an information category replacing the image data file with a matrix of specific classes. Each pixel is characterized by its spectral signature, which is determined by the relative reflectance in different wavelength bands. Thus, multispectral classification is an information extraction process that analyses these signatures and assigns pixels to classes based on similar signatures.

Data merging includes procedures to combine image data for a given area with other data sets for the same area. Regarding satellite imagery, image fusion is the combination of two or more different images to form a new image by using a certain algorithm. The image resulting from this process contains more information than the original. Specifically, fusion of a multispectral image of relatively low spatial resolution with a high resolution panchromatic image is called pan-sharpening and it is an important issue for a number of remote sensing applications of large scale (Zhang 2004). Several image fusion techniques have been developed trying to combine spectral information of the multispectral image with spatial information of



the panchromatic image. Depending on the application, as well as on the computer-based analysis that will follow (e.g. classification), attention should be paid in the selected fusion method in order to obtain better preservation of the spectral characteristics (Karagianni and Lazaridou 2017).

Visual analysis is also a key element in the interpretation of the initial satellite data, as well as in every step of digital image processing and often depends on the techniques to be followed. Different land cover features (water, soil, vegetation, concrete, snow, etc.) reflect visible and infrared light in different ways. Interpretation of optical images requires the knowledge of the spectral reflectance patterns of various materials (natural or man-made) covering the surface of the earth.

To detect and delineate the area affected by the landslide in this case study, several methods can be applied. Initially, different color composites can be used to highlight several features in the landscape and reveal the bare ground or vegetation allowing the interpreter to detect the presence of landslides. Spectral bands capture energy in different parts of the electromagnetic spectrum. Using different band combinations certain features will contrast greatly with their surroundings, enabling better delineation (Scaioni et al. 2014).

Further digital image processing techniques (spectral enhancement, pan-sharpening, image algebra, etc.) can be applied for change detection and direct landslide monitoring (Hervás et al. 2003; Joyce et al. 2009; Scaioni et al. 2014). Visual interpretation of images (before or/and after digital processing) taken at different times can also contribute to the qualitative analysis of change detection (Scaioni et al. 2014) and is being done on the base of geometric (shape, size, etc.) and radiometric (tone-color, texture) characteristics. Optical data can provide good results due to spatial resolution and sensor look angle (although misclassification in other areas of bare ground may appear) (Joyce et al. 2009; van Westen 2000).

The software that was used for digital processing of the satellite imagery is ERDAS Imagine 2011 and SNAP (Sentinel Application Platform) freely distributed by ESA (STEP-Scientific Toolbox Exploitation Platform 2018).

## ***7.1 Landsat 8 Image Processing***

Digital processing of Landsat 8 data included layerstacking of the downloaded data, subsetting the scene to the study area, spectral enhancement performing principal components analysis (PCA) and image fusion (pan-sharpening) using Wavelet transform.

As a first step, various color composites can be used to visualize the information in the bands of the acquired images. In this study, the band combinations that were considered the most effective for a qualitative approach of the landslide detection were the following: the Natural Color Composite 4-3-2 (Red: Band 4, Green: Band 3, Blue: Band 2) and the Color Composite 6-3-2 (Red: SWIR1-Band 6, Green: Band 3, Blue: Band 2). These band combinations were applied at the images

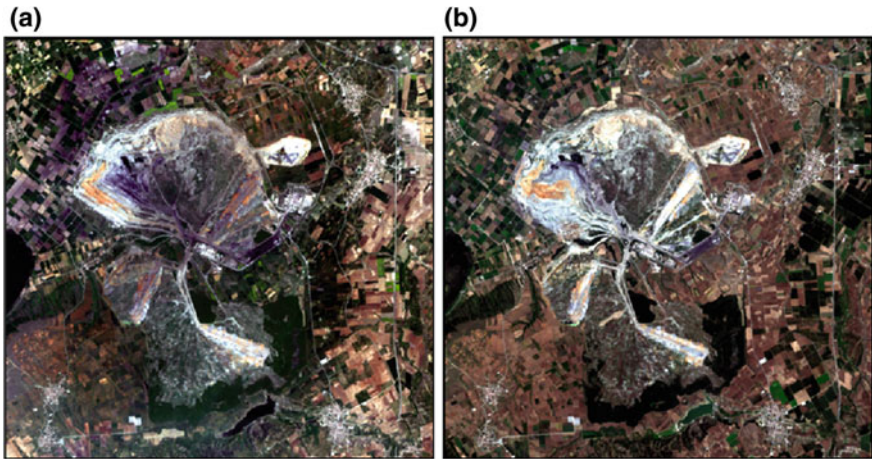


**Fig. 13** Study area in Natural Color Composite (4-3-2) before (a) and after (b) the landslide

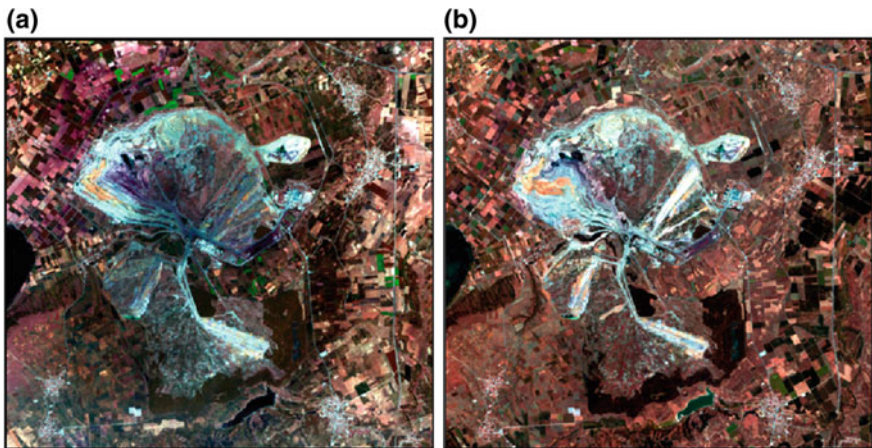


**Fig. 14** Study area in Color Composite (6-3-2) before (a) and after (b) the landslide

acquired before (02-05-2017) and after (26-06-2017) the event and were visually compared.

In the Natural Color Composite 4-3-2 (Fig. 13) ground features appear in colors similar to their appearance to the human visual system. The landslide area is detected in the left part of the mine and the slope deformations are visible. In the Color Composite 6-3-2 (Fig. 14), the landslide area is also detected and clearly highlighted, as the shortwave infrared band (SWIR1) that were used in this combination is suitable for discerning differences in bare earth, indicating wet and dry areas in a scene.

Further digital processing concerned spectral enhancement of the satellite images, applying principal components analysis (PCA). This statistical method of data compression allows redundant data to be compacted into fewer bands. Dimensionality of the data set is reduced by projecting the data along new non-correlated axes. The bands of PCA data (principal components-PCs), are non-correlated and independent, therefore are often more interpretable than the source data (ERDAS Field Guide 2013, Deng et al. 2008). Although there are  $n$  output bands in a PCA, the first few bands account for a high proportion of the variance in the data. This image enhancement technique is useful for compressing data into fewer bands and can be used to give satisfactory results in change detection analysis, as in several applications appears to be better than classification comparison approach for change detection (Gupta et al. 2013).

There are several ways to apply PC transformation for change detection (Deng et al. 2008). In this study, to detect changes that appeared after the landslide, Landsat 8 images of two different times were both transformed into new PCA images applying PC transformation and were compared visually (Fig. 15). Most of the variance of the dataset is found on the first components. Therefore, the first three images are presented (3 principal components: PC1, PC2, PC3) as they provide most of the information contained within the dataset. The results were evaluated visually.

Areas affected by the landslide are evident in all three components. In PC1 pair of images the landslide area appears in lighter shades of grey while built up areas and water regions are also highlighted. In PC2 pair of images landslide area appears in darker shades and vegetation regions are discernible. In PC3 pair of images the 'boundaries' of the lignite mine are delineated and especially the landslide area in the left part of the mine (lighter shades of grey) where a shape disturbance is detected.

To exploit the panchromatic band of Landsat 8 (spatial resolution: 15 m) image fusion (pan-sharpening) was performed in order to delineate the landslide area in more detail. Various methods have been developed for image fusion. In this study, Discrete Wavelet transform (DWT) was chosen as in several cases seem to preserve better the spectral characteristics of the original multispectral image and can be more effective for further digital processing (Karagianni and Lazaridou 2017; Gungor and Shan 2004).

Wavelet methods belong in the broader category of Multiple Resolution Analysis (MRA) methods. In wavelet fusion, a high resolution panchromatic image is first decomposed into a set of low resolution panchromatic images using corresponding wavelet coefficients (spatial details) for each level. Individual bands of the multispectral image then replace the low resolution panchromatic image at the resolution level of the original multispectral image. The high resolution spatial detail is injected into each multispectral band by performing a reverse wavelet transform on each multispectral band using the corresponding wavelet coefficients (Zhang 2004).

The pansharpened images are presented in Fig. 16 focusing in the affected area (left part of the mine) and are evaluated visually, as well as quantitatively.

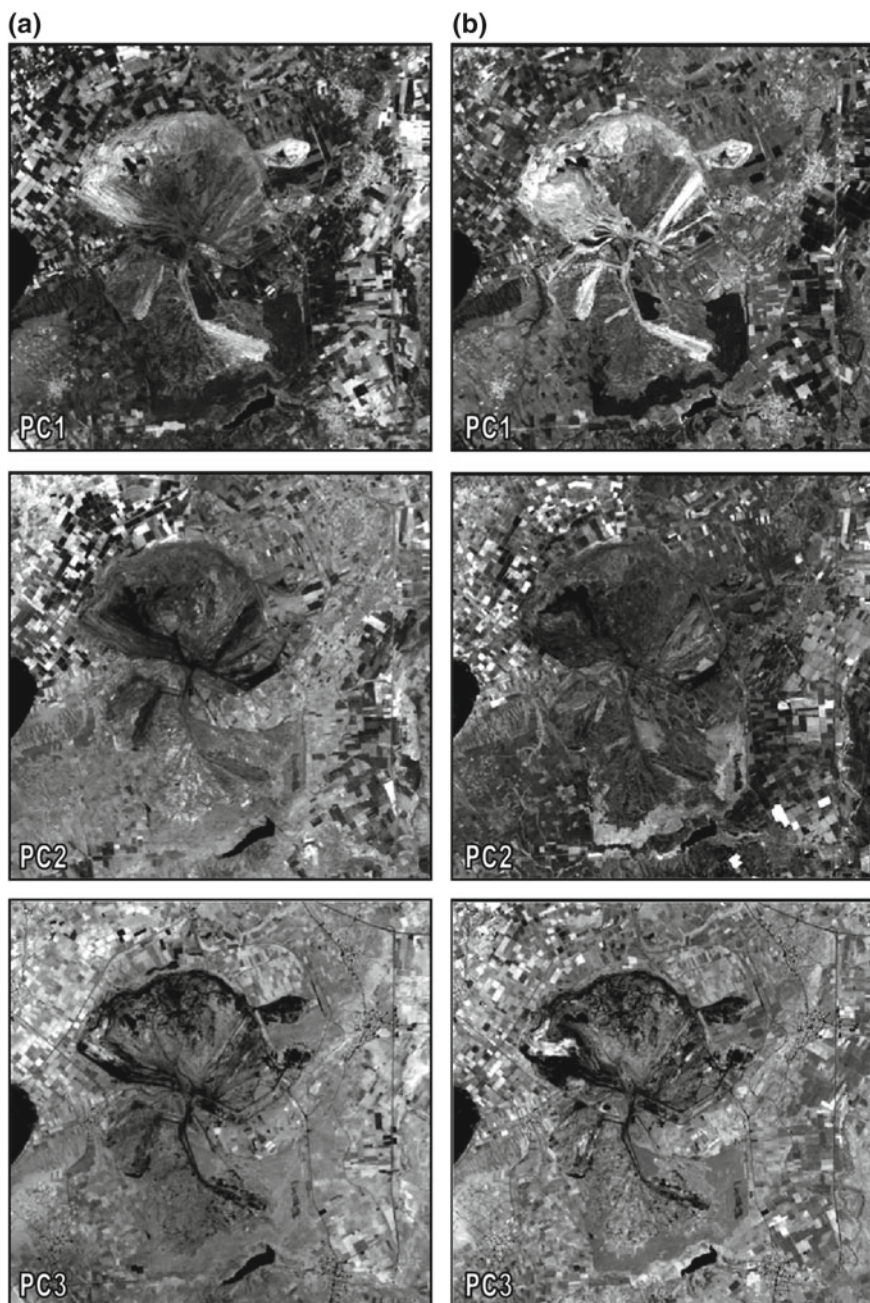


**Fig. 15** PCA images of the study area before (a) and after (b) the landslide

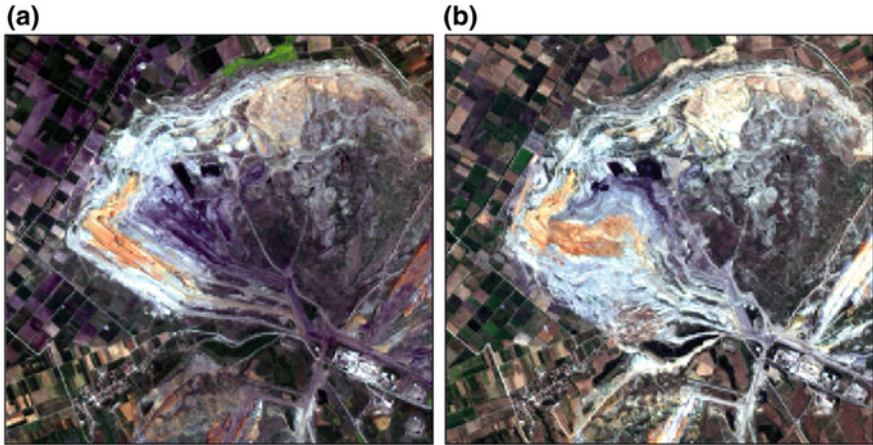


**Fig. 16** Pansharpened images of the study area in Natural Color Composite (4-3-2) before (a) and after (b) the landslide

As is presented in Fig. 16, the spatial resolution of the images after pan-sharpening is improved and the landslide area is distinguished in more detail. In addition, there is a minimum color distortion regarding the original multispectral images. Therefore, the resulted images are suitable for change detection as spectral information is maintained while at the same time spatial resolution is increased.

In order to evaluate quantitatively the pansharpened images for both dates, the correlation coefficients among the Landsat 8 multispectral bands before and after pan-sharpening were calculated. The results are presented in Table 1, indicatively

**Table 1** Correlation coefficients among the Landsat 8 multispectral bands before and after pan-sharpening (for both dates and indicatively for bands 2, 3, 4)

02-05-2017		Band 2	Band 3	Band 4
Band 2	Before	1	0.964	0.878
	After	1	0.963	0.877
Band 3	Before	0.964	1	0.940
	After	0.963	1	0.939
Band 4	Before	0.878	0.940	1
	After	0.877	0.939	1
26-06-2017		Band 2	Band 3	Band 4
Band 2	Before	1	0.974	0.899
	After	1	0.973	0.898
Band 3	Before	0.974	1	0.945
	After	0.973	1	0.944
Band 4	Before	0.899	0.945	1
	After	0.898	0.944	1

for bands 2, 3, 4. An acceptable fusion approach should not present considerable changes in the correlation of the corresponding bands (Gungor and Shan 2004). As shown in Table 1, the correlation among all bands is subject to minor changes after applying Wavelet transform. In addition, high spectral value preservation is observed, as values are close to +1.

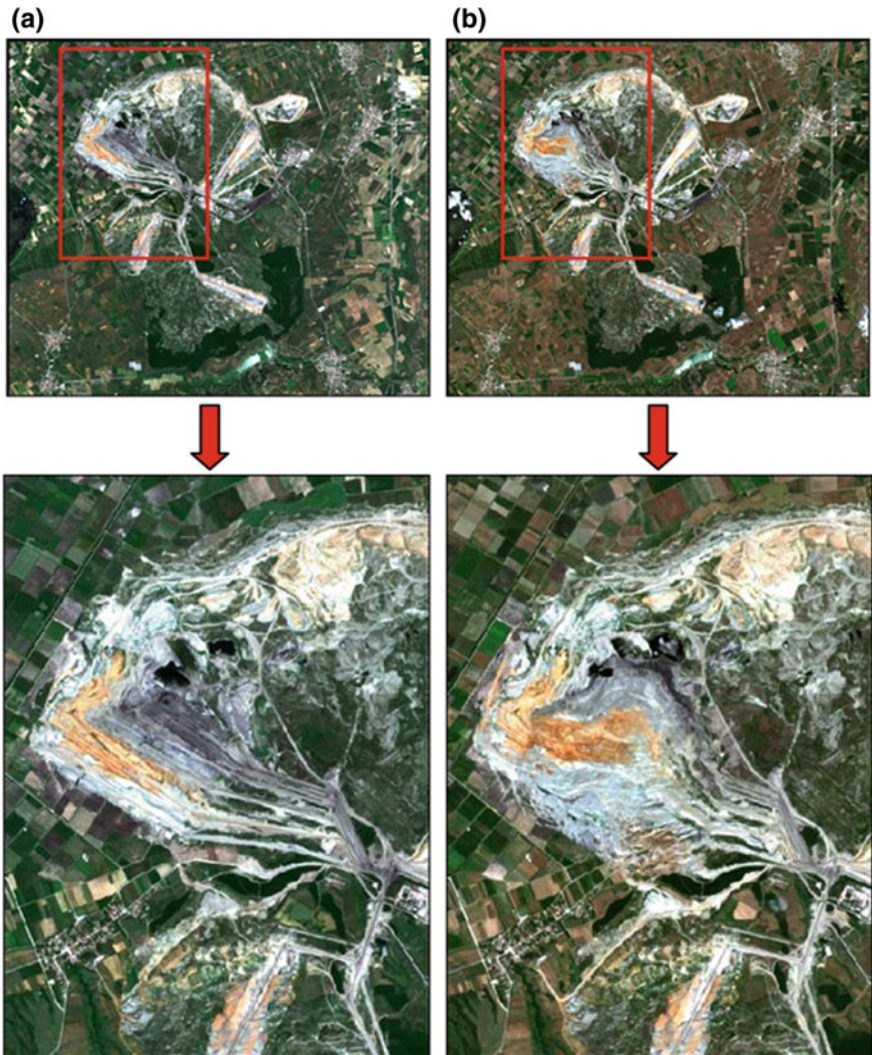


**Fig. 17** Sentinel-2A images of the study area in Natural Color Composite (4-3-2) before (a) and after (b) the landslide

## 7.2 Sentinel-2A Image Processing

Digital processing of Sentinel-2A data included resampling at 10 m, layerstacking of the downloaded data, subsetting the scene to the study area and image algebra technique implementation (image difference) to detect the changes.

Figure 17 presents the study area before and after the landslide in Natural Color Composite (4-3-2), as well as a second pair of subsets that focuses on the left area of the mine where the landslide occurred (red rectangle in the first pair of images).

Visual interpretation of Sentinel-2 images could prove to be more effective than interpretation of Landsat 8 images due to higher spatial resolution of the former (10 m vs. the 30 m of Landsat 8). In addition, relevant indicators as texture, vegetation density, land use, cracks, surface disturbance or scarp visibility could be used to detect the presence of landslides. As shown in the second pair of images in Fig. 17 the affected area is clearly detected and difference in texture as well as surface disturbance are also evident.

To exploit further the high spatial resolution that Sentinel-2 offers (10 m after resampling), as well as the processing level of the data (L2A data are atmospherically corrected) an image algebra change detection technique (image difference) was applied to detect spectral reflectance differences between the two images.

Image difference is an image-to-image comparison and can be used for change analysis with images that depict the same area at different points in time. This process computes the differences between two images, highlighting change that



**Fig. 18** Resulted image after applying ‘image difference’

exceeds a user-specified threshold (ERDAS Field Guide 2013). The first image (before the event) is subtracted from the second image (after the event). Any changes in brightness values over time are reflected in the resulted grayscale image. Selecting a threshold value to express the changes in brightness as a percent, increases or decreases in brightness values that are greater than this threshold will be highlighted in certain color. Familiarity with the study area could help to place the critical threshold properly between true changes and spurious changes. The final product is a thematic image.

The resulted thematic image after applying image difference in Sentinel-2A images is presented in Fig. 18. The red color represents the changes detected in brightness values (increases or decreases) regarding the images that are compared (before and after the landslide). The processing was limited in an area of interest according to the previous findings (landslide area detection in the left part of the lignite mine).

## 8 Discussion–Conclusions

Natural or man-made disasters are phenomena that can affect large areas and have many impacts (environmental, societal and economic). Landslides are among the major disasters of large scale that may affect the natural environment as well as urban areas, often causing massive destruction, loss of property, or even fatalities worldwide. Developing tools that are effective for disaster management is imperative to monitor and mitigate their effect. Satellite data and remote sensing techniques, combined with geological data and studies can provide valuable information regarding monitoring of natural hazards in general and especially of landslides.

In this chapter, Landsat 8 and Sentinel-2 satellite data were used to study a complex set of landslides that occurred in the lignite mine of Amynteon in north-western Greece. The landslide occurred in along the south faces of the mine, resulting to extended collapses, destruction of mining machinery, evacuation of the adjacent Anargyri village and a big financial impact. Digital image processing techniques were applied for change detection in satellite data acquired before and after the event and geological data were also used to provide information about the geological background of the area and landslides vulnerability.

According to geological data, this is probably a multifactor event. It is possible that the multifragmented Plio-Pleistocene sedimentary sequence, due to the transfer zone between the Anargyri and Vegora marginal fault zones acted as a soil, instead of a rock, mass. These fault zones affected the lignite bearing formations, causing poor cohesion. Due to widespread fragmentation of the lignite-bearing sequence the mine landslide shows characteristics of a rotational landslide. It is also possible that human factors affected the initiation of the landslide. Hydrogeological factors that predated the event had already been identified in previous studies (e.g. Tzampoglou and Loupasakis 2016), while, a few days before the main landslide a heavy rainfall



was recorded during a normally dry period, possibly accelerating the already initiated earth mass movements.

Regarding digital processing of Landsat 8 data, different color composites along with spectral enhancement (principal components analysis-PCA) were used to detect the changes and delineate the landslide. Spectral capabilities of the data gave the opportunity to identify the location, as well as the extent of the landslide. Applying PCA, data were compressed into fewer bands and the resulted images (first three components) were visually interpreted giving satisfactory results in change detection analysis.

In order to delineate the landslide area in more detail a Wavelet transform was applied to combine the rich spectral context of the multispectral images with the high spatial resolution of the panchromatic image (pan-sharpening). The pan-sharpened images were effectively evaluated visually, as well as quantitatively. They can be photointerpreted easier than the original, while preservation of the spectral characteristics makes them suitable for change detection.

Sentinel-2A satellite data were also used as they were considered effective for change detection analysis due to high spatial resolution (higher than this of Landsat 8 data, even after pan-sharpening), data acquisition frequency and policy of free data (as Landsat 8 data). Visual interpretation of Sentinel-2 images provides more details about the affected area as differences in texture and surface disturbance are clearly detected.

To exploit further the high spatial resolution of Sentinel-2 atmospherically corrected data (Level-2 products) an image algebra technique (image difference) was applied to detect spectral reflectance differences between the two images. The resulted thematic image that reflects changes in brightness values of the pixels provides useful information about the parts of the lignite mine that are affected and could contribute further to landslide monitoring. Direct digital processing for change detection may limit the uncertainty of outputs, as well as the subjectivity and the strict dependency on human expertise that visual interpretation introduces.

Further processing extension could include a combination of SAR and optical data. SAR data could be a further step in digital processing (displacement calculations and volume estimation), especially in scenes where cloud cover impedes optical acquisition. Moreover, terrestrial laser scanning (TLS) systems could be used to generate 3D point clouds and DEMs of the area contributing to landslide monitoring. Complementary ground-based techniques could also be used to acquire precise information on displacement or deformation at specific locations, especially near residential areas and road infrastructure.

## References

- Chatzipetros A (1998) Palaeoseismological and morphotectonic study of the Mygdonia, Eastern Halkidiki and Kozani-Grevena active fault systems. PhD thesis, Aristotle University of Thessaloniki (in Greek)
- Copernicus Open Access Hub (2018). <https://scihub.copernicus.eu>. Accessed 23 Sept 2018
- Deng JS, Wang K, Deng YH, Qi GJ (2008) PCA-based land-use change detection and analysis using multitemporal and multisensor satellite data. *Int J Remote Sens* 29(16):4823–4838

- Dimitrakopoulos D, Koumantakis I (2017) Hydrodynamic regime of Amynteon basin. Influence of open lignite mines. Paper presented at the 11th international hydrogeological congress of Greece, Athens, Greece, 4–6 Oct 2017
- Dong Y, Fu B, Ninomiya Y (2009) Geomorphological changes associated with underground coal mining in the Fushun area, northeast China revealed by multitemporal satellite remote sensing data. *Int J Remote Sens* 30(18):4767–4784
- EarthExplorer (2018). <http://earthexplorer.usgs.gov>. Accessed 23 Sept 2018
- ERDAS Field Guide™ (2013) Intergraph Corporation, Erdas Inc., U.S.A 405, 440–445, 453–454
- Gili JA, Corominas J, Rius J (2000) Using Global Positioning System techniques in landslide monitoring. *Eng Geol* 55(3):167–192
- Google Earth (2018). <https://www.google.com/intl/el/earth>. Accessed 23 Sept 2018
- Gungor O, Shan J (2004) Evaluation of satellite image fusion using wavelet transform. Paper presented at the XX th ISPRS Congress, Istanbul, Turkey, 12–23 July 2004
- Gupta RP, Tiwari RK, Saini V, Srivastava N (2013) A simplified approach for interpreting principal component images. *Adv Remote Sens* 2:111–119
- Hervás J, Barredo JI, Rosin PL, Pasuto A, Mantovani F, Silvano S (2003) Monitoring landslides from optical remotely sensed imagery: the case history of Tessina landslide, Italy. *Geomorphology* 54:63–75
- Interactive database Meteosearch (2018). <http://meteosearch.meteo.gr/data/amyntaio/2017-06.txt>. Accessed 23 Sept 2018
- Joyce KE, Belliss SE, Samsonov SV, McNeill SJ, Glassey PJ (2009) A review of the status of satellite remote sensing and image processing techniques for mapping natural hazards and disasters. *Prog Phys Geogr* 33:183–207
- Karagianni A, Lazaridou M (2017) Fusion of multispectral and panchromatic satellite images in environmental issues. *Int J Eng Res Appl* 7(7):47–50
- Kiliass A, Mountrakis D (1989) The tectonic nappe of Pelagonian zone: tectonics, metamorphism and magmatism. *Bull Geol Soc Greece* 23:29–46 (in Greek)
- Landsat 8 Mission (2018). <http://landsat.usgs.gov/landsat8.php>. Accessed 23 Sept 2018
- Li Y, Zhao H, Fan J (2015) Application of remote sensing technology in mine environment monitoring. Paper presented at the international conference on engineering technology and application (ICETA), Taipei, Taiwan, 22–24 April 2015
- Lillesand TM, Kiefer RW (1987) Remote sensing and image interpretation, 2nd edn. John Wiley and Sons, New York
- Mantovani F, Soeters R, Van Westen CJ (1996) Remote sensing techniques for landslide studies and hazard zonation in Europe. *Geomorphology* 15:213–225
- Metternicht G, Humi L, Gogu R (2005) Remote sensing of landslides: an analysis of the potential contribution to geo-spatial systems for hazard assessment in mountainous environments. *Remote Sens Environ* 98:284–303
- Mountrakis D (1986) The pelagonian zone in Greece: a polyphase-deformed fragment of the cimmerian continent and its role in the geotectonic evolution of the eastern Mediterranean. *J Geol* 94:335–347
- Navi K (2017) Satellite image processing. In: Proceedings of the fourth international conference on signal processing, communication and networking (ICSCN), Chennai, India, 16–18 March 2017
- Paul D, Banks G, Ballard C, Gillieson D (2006) Monitoring the environmental impact of mining in remote locations through remotely sensed data. *Geocarto Int* 21:33–42
- Pavlidis S (1985) Neotectonic evolution of Florina–Vegoritida–Ptolemais basin. PhD thesis, Aristotle University of Thessaloniki (in Greek)
- Pavlidis S, Mountrakis D (1987) Extensional tectonics of northwestern Macedonia, Greece, since the Late Miocene. *J Struct Geol* 9:385–392
- Pavlidis SB, Zouros NC, Chatzipetros AA, Kostopoulos DS, Mountrakis DM (1995) The 13 May 1995 western Macedonia, Greece (Kozani-Grevena) earthquake; preliminary results. *Terra Nova* 7:544–549

- Scaioni M, Longoni L, Melillo V, Papini M (2014) Remote sensing for landslide investigations: an overview of recent achievements and perspectives. *Remote Sens* 6:5909–5937
- Sentinel-2 Mission (2018). <https://sentinel.esa.int/web/sentinel/missions/sentinel-2>. Accessed 23 Sept 2018
- STEP-Scientific Toolbox Exploitation Platform (2018). <https://step.esa.int>. Accessed 23 Sept 2018
- Tsapanos T (2005) Seismicity and seismic hazard in western Macedonia. *Bull Geol Soc Greece* 37:232–244
- Tzampoglou P, Loupasakis C (2016) New data regarding the ground water level changes at the Amyntaio basin–Florina Prefecture, Greece. *Bull Geol Soc Greece* 50:1006–1015
- Tzampoglou P, Loupasakis C (2017a) Mining geohazards susceptibility and risk mapping: the case of the Amyntaio open-pit coal mine, West Macedonia, Greece. *Environ Earth Sci* 76:542
- Tzampoglou P, Loupasakis C (2017b) Updated ground water piezometry data of the Amyntaio sub-basin and their effect on the manifestation of the land subsidence phenomena. Paper presented at the 11th international hydrogeological congress of Greece, Athens, Greece, 4–6 Oct 2017
- Tzampoglou P, Loupasakis C (2018) Evaluating geological and geotechnical data for the study of land subsidence phenomena at the perimeter of the Amyntaio coalmine, Greece. *Int J Min Sci Technol* 28:601–612
- USGS (2018) U.S. Geological Survey. <https://pubs.usgs.gov>. Accessed 23 Sept 2018
- van Westen C (2000) Remote sensing for natural disaster management. *Int Arch Photogramm Remote Sens XXXIII(Part B7):1609–1617*
- Wang Q, Guo H, Chen Y, Lin Q, Li H (2013) Application of remote sensing for investigating mining geological hazards. *Int J Digit Earth* 6(5):449–468
- Zhang Y (2004) Understanding image fusion. *Photogramm Eng Remote Sens* 657–661